Analytical modeling of orientation effects in random nanowire networks

Milind Jagota ⬤* and Isaac Scheinfeld ⬤†
Stanford University, Stanford, California 94305, USA

Films made from random nanowire arrays are an attractive choice for electronics requiring flexible transparent conductive films. However, thus far there has been no unified theory for predicting their electrical conductivity. In particular, the effects of orientation distribution on network conductivity remain poorly understood. We present a simplified analytical model for random nanowire network electrical conductivity that accurately captures the effects of arbitrary nanowire orientation distributions on conductivity. Our model is an upper bound and converges to the true conductivity as nanowire density grows. The model replaces Monte Carlo sampling with an asymptotically faster computation and in practice can be computed much more quickly than standard computational models. The success of our approximation provides theoretical insight into how nanowire orientation affects electrical conductivity.

I. INTRODUCTION

Transparent conductive films are a crucial component of touch screens and solar cells, among various other electronics [1,2]. One approach to making transparent conductive films that has been widely studied and deployed is to randomly disperse highly conductive nanowires into a substrate. Films made in this way, using conductive material such as silver nanowires or carbon nanotubes, display competitive electrical and optical properties to alternatives, while being cheaper and more flexible than the performance standard indium tin oxide [3–7]. The latter property is particularly valuable as flexible electronics continue to become more mainstream in consumer devices. However, despite the wide interest in applying them, there is no unified theory for predicting electrical properties of random nanowire networks, and many observed effects have not been fully characterized or explained. As a result, the technology remains underdeveloped, and there is undoubtedly still room for improvements in performance.

The majority of results describing properties of random nanowire networks have been experimental or via direct computational simulation. Various studies have experimentally compared electrical properties of films using different conductive rods, such as silver nanowires and carbon nanotubes [4,5,8]. Agreement between simulation and experimental observations of electrical properties has also been well established for the classes of random nanowire networks that are easiest to produce experimentally [9]. More recently, computational models have been used to maximize electrical performance of random nanowire networks by varying the distributions from which the networks are sampled [10–17]. Some of these results have been verified experimentally [18–21]. In particular, various computational studies have demonstrated that it is possible to improve

electrical conductivity of nanowire networks by controlling nanowire orientation [10–16]. However, this effect is not well understood, and there is no simple framework to predict the result of using a specific, arbitrary orientation distribution.

Recently, a number of analytical models have also been developed to describe properties of random nanowire networks, but none thus far have explained the effect of nanowire orientation on electrical conductivity in full generality [22–29]. Forro *et al.* proposed a model derived assuming high nanowire density, so that potential drop across nanowire networks can be assumed to be linear [25]. The model is accurate in the high-density regime and yields a closed-form expression. Benda *et al.* obtained a closed-form expression for network conductivity by numerically fitting a physically interpretable form to Monte Carlo simulations, while Manning *et al.* developed a theoretical framework for analyzing both electrical and optical performance of nanowire networks [26,28]. However, these models are developed under the assumption of uniformly distributed wire orientation and do not generalize in a clear manner to random orientation of an arbitrary distribution.

In this work, we present an analytical model for random nanowire network conductivity that accurately captures the effects of arbitrary distributions of nanowire orientation. Our approximate model replaces Monte Carlo sampling with an asymptotically less expensive computation and is empirically much faster than standard computational models. It approaches the limiting dependency of network conductivity on nanowire density, with small errors even at moderate nanowire densities. Furthermore, the structure of our approximations provides intuition for how orientation affects network conductivity as well as intuition for the behavior of random nanowire networks in general.

II. MODEL CONSTRUCTION

A. Setting

We begin by presenting the setting in which we develop our model. We consider networks comprising one-dimensional

---

*Corresponding author: mjagota@stanford.edu
†ischeinfeld@stanford.edu

nanowires (linear, widthless sticks) inside a square space of unit length in each direction with periodic boundary conditions at the top and bottom. To simplify notation, we assume nanowires have fixed length l, but our approach generalizes naturally to having a random distribution over wire length. Each nanowire is described by an (x, y) coordinate pair and an angle θ, where the coordinate pair represents the location of the wire center and θ is the angle relative to the horizontal. The coordinates and the angle are sampled randomly, where all values are assumed independent and each nanowire in a network is assumed to be independent. We denote the sampling distributions of x, y, θ by $\mathcal{X}, \mathcal{Y}, \Theta$, respectively.

The primary electrical property of interest for random nanowire networks is the sheet conductivity σ, which is a random variable. Sheet conductivity transitions sharply from being zero with overwhelming probability to being greater than zero with overwhelming probability at a particular number of nanowires that is a function of l, known as the percolation threshold [30]. The dimensionless quantity

$$C_N := N|l|^2, \tag{1}$$

where N is the number of nanowires in an network and $|l|$ indicates the wire length normalized by dividing by box width, is often used as a normalized concentration of nanowires because it allows direct comparison to the percolation threshold [10]. We assume that our nanowire networks are well above the percolation threshold so that they are guaranteed to have conductivity greater than zero. We focus on modeling the expected value of the sheet conductivity $E\sigma$, because the variance of sheet conductivity is typically small relative to the expected sheet conductivity for large N [9,10].

Figure 1 displays how the sheet conductivity is physically defined, using a network sampled with nanowire positions and orientations both distributed uniformly. We place electrodes at the left and right boundary of the network ($x = 0$ and $x = 1$) and calculate the current when 1 V is applied. This current can then be used to calculate the sheet conductivity. In general, there are three sources of resistance in nanowire networks which determine the conductivity along with the geometry: the resistance of wires themselves, the resistance at the junctions between two wires, and the resistance at the junctions between a wire and an electrode. In many real nanowire networks, the wire resistance is small compared to the resistance at junctions [9]. We assume that this is the case and choose to ignore the wire resistance moving forward. However, our method can be generalized to account for wire resistance, and we discuss this in Sec. V. We set the resistance between two wires to be a constant 1Ω and set the resistance between a wire and an electrode to be a constant $\frac{1}{100}\Omega$. The conductivity of a particular network is determined solely by the ratio between these two quantities up to scaling. We expect the wire-wire resistance to be multiple orders of magnitude larger than the wire-electrode resistance, and these quantities are thus reasonable.

In this setting, σ can be calculated exactly for a particular network from the symmetric $(N + 2) \times (N + 2)$ adjacency matrix of the electrical network, which we denote as A. The first N rows of this matrix each corresponds to a single wire, while the last two rows correspond to the left and right border electrode. An off-diagonal element of the matrix is 1 if the two
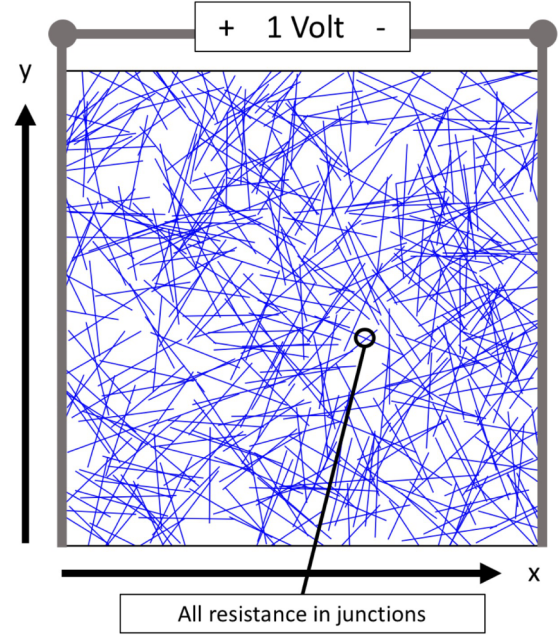

FIG. 1. The sheet conductivity of a nanowire network is calculated by computing the current when 1 V is applied by electrodes spanning the left and right border of the network. We assume that nanowire network resistance is dominated by junction resistance and ignore wire resistance. The x direction is defined as the direction of current flow, and the y direction is perpendicular.

corresponding objects touch, and all diagonal elements are 0. From A, we can use the two resistance values to construct the Laplacian matrix of the nanowire network L, of the same shape as A. This is the matrix that, when multiplied by the vector of node voltages V, gives the vector of node net current flow J as given in Eq. (2) and is a linear function of A [31]:

$$LV = J. \tag{2}$$

We can then calculate the current flowing from the left electrode by setting the voltages at the left and right electrodes in the vector V and solving for the remaining voltages. Dividing this current by the applied voltage yields the sheet conductivity [31].

B. Model definition

The expected sheet conductivity $E\sigma$ has most often been studied by direct sampling of nanowire networks [9–17]. This procedure involves numerous steps. For each network, N nanowires are sampled according to the distributions $\mathcal{X}, \mathcal{Y}, \Theta$. Then the adjacency matrices A for the networks are generated. From these matrices, observations of the sheet conductivity can be calculated by applying Kirchhoff's laws, which are then averaged to yield an estimate. We denote this empirical estimate by $\hat{\sigma}$, defined in Eq. (3), where $\sigma(A_i)$ refers to the sheet conductivity of the network represented by the adjacency matrix A_i:

$$\hat{\sigma} = \frac{1}{M} \sum_{i=1}^{M} \sigma(A_i). \tag{3}$$

While this approach converges rapidly to $E\sigma$ as the number of sampled networks M increases, it has a number of drawbacks. First, it is slow: calculating the adjacency matrix A from a list of wire coordinates and angles requires checking all pairs of nanowires for intersection, as well as computing a Cholesky decomposition of an $N \times N$ matrix. While there are methods to speed up both of these steps, the procedure is still at least $O(MN^2)$, and so collecting many samples for high conductivity films is slow. In addition, this sampling-based procedure makes interpretation of observed effects difficult, which limits physical intuition.

An exact analytical model for the sheet conductivity would fix these issues, but directly deriving an expression for $E\sigma$ is very difficult even under the simplest distributions $\mathcal{X}, \mathcal{Y}, \Theta$. A common approximation for this type of problem is to move the expectation inside of the complicated function, as shown in Eq. (4). The right side of this equation is defined by treating EA as a weighted adjacency matrix; the Laplacian L is constructed from EA by the same linear relationship as for an ordinary adjacency matrix A, and the sheet conductivity is calculated by solving the same matrix equation involving L:

$$E\sigma(A) \approx \sigma(EA). \qquad (4)$$

However, this naive approach fails catastrophically for random nanowire networks. None of the spatial structure of the networks is captured because all nanowires are indistinguishable according to EA. Using $\sigma(EA)$ as a model results in a massive overestimate of the sheet conductivity that is not useful.

To develop our analytical model, we modify the approach of moving the expectation inside the function to directly capture spatial structure of random nanowire networks. We first observe that σ is clearly invariant to reindexing the wires in a network and recalculating the adjacency matrix A accordingly. We choose to assume, without loss of generality, that the wires are always reindexed according to increasing x coordinate. Specifically, define the random matrix A^* as

$$A^*_{\text{rank}(i),\text{rank}(j)} = A_{ij}, \qquad (5)$$

where the function rank(i) gets the placement of x_i in the list of x coordinates when sorted from smallest to largest and leaves the electrode indices fixed. Our approximate model σ^* is then defined in Eq. (6), where $\sigma(EA^*)$ is defined in the same way as the right side of Eq. (4):

$$\sigma^* := \sigma(EA^*). \qquad (6)$$

Under slightly more restrictive assumptions, we can prove that σ^* is greater than $E\sigma$ for all $\mathcal{X}, \mathcal{Y}, \Theta$ using Jensen's inequality; details are presented in Sec. II C. Despite being an upper bound, σ^* is able to capture the dependency of conductivity on both wire concentration and orientation distribution due to the choice of assumed wire permutation; EA^* encodes most of the relevant spatial structure of the networks. We illustrate this property of our model in Fig. 2 by plotting the values of a random sorted adjacency matrix A^* as well as the values of EA^* under the same distributions. Due to the sorted order that is assumed, the matrices A^* for sampled random networks are banded, because wires near in index are also near in x coordinate and therefore more likely to intersect. The
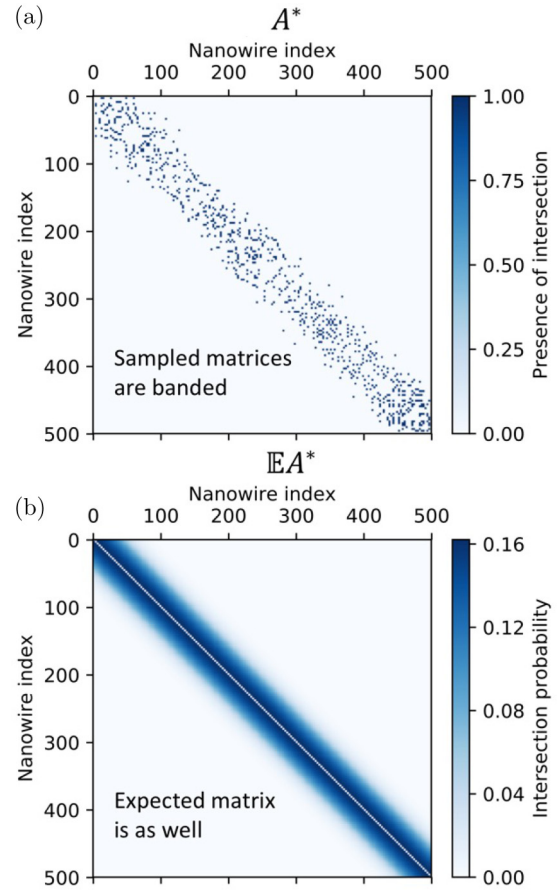

FIG. 2. The values of (a) the sorted adjacency matrix A^* of a random nanowire network and (b) the sorted expected adjacency matrix EA^* for the distributions that the sample was drawn from, with $N = 500$ and $l = 0.2$. The sampled matrix is banded with elements equal to 0 or 1, with 1 indicating an intersection between the corresponding nanowires. The expected matrix has elements equal to the probability of intersection between the corresponding nanowires and captures the banded structure of the sampled matrices A^*. EA^* has a small maximum value because even if two nanowires have no x separation, the probability of them intersecting is small when l is small.

expected adjacency matrix EA^* reproduces this key property well.

In the true system, nanowires that intersect are close in y coordinate as well as in x coordinate. We encode this effect only with respect to x coordinate and not y coordinate, but our empirical results verify that our model is useful regardless. This result has interesting implications which we discuss in Sec. IV.

C. Proof that σ^* is an upper bound

We argue that σ^* is an upper bound on $E\sigma$ under slightly more restrictive assumptions. Note that the Laplacian matrix L for a particular nanowire network is a linear function of the sorted adjacency matrix A^* [31]. It satisfies the Kirchhoff current equation given in Eq. (2), where V is the vector of voltages at each of the $N + 2$ objects and J, the net current flowing into each node, is zero at all nodes other than the electrode nodes. To reduce notation for units, we assume in

this section that V is made dimensionless by dividing each element by 1 V. L and J then both have units of inverse resistance.

Under the assumed normalization of V, the sheet conductivity is equal to the current flowing out of the left border electrode (node $N + 1$) when we set the voltage at the left border to be 1 V and the voltage at the right border to be 0 V ($V_{N+1} = 1$, $V_{N+2} = 0$). With these values of V set, the Kirchhoff current equation is given by Eq. (7):

$$L_{1:N,1:N}V = -L_{1:N,N+1}. \quad (7)$$

We use the notation $B_{i:j,k:l}$ to refer to the submatrix of B from rows i to j and columns k to l. A single index indicates taking a single row or column.

We proceed by adding two minor assumptions. We first assume that for fixed distributions $\mathcal{X}, \mathcal{Y}, \Theta$, the number of nanowires crossing the left electrode is a constant integer M. For the high-density networks we study, the variance of this quantity is small with respect to its expected value and does not cause much variance in sheet conductivity. Second, we assume that the M nanowires that cross the left border are the first M indices in A^*. Under the sorting that is used for A^*, this is the most likely set of M wires to cross the left border, and the variance of these indices also does not cause much variance in sheet conductivity. This assumption can be viewed as a definition of sheet conductivity where we attach our left electrode to the leftmost M wires based on center location, as opposed to based on left endpoint location.

Under these assumptions, the sheet conductivity is given by Eq. (8), where R_{ew} is the wire-electrode resistance in ohms and E_M is the N dimensional vector that is 1 in the first M elements and 0 otherwise:

$$
\begin{aligned}
\sigma &= \frac{1}{R_{ew}} \sum_{i=1}^{M} (1 - V_i) \\
&= \frac{1}{R_{ew}} \left(M - \sum_{i=1}^{M} V_i \right) \\
&= \frac{1}{R_{ew}} \left(M - E_M^T V \right) \\
&= \frac{1}{R_{ew}} \left\{ M + \left[E_M^T (L_{1:N,1:N})^{-1} L_{1:N,N+1} \right] \right\}. \quad (8)
\end{aligned}
$$

The inverse of $L_{1:N,1:N}$ exists when the network is connected, which is true because we assume that our networks are well above the percolation threshold.

Since the first M nanowires cross our left measurement electrode, $L_{1:N,N+1}$ is given by

$$L_{1:N,N+1} = -\frac{1}{R_{ew}} E_M. \quad (9)$$

We can use this value to write another expression for σ in Eq. (10):

$$\sigma = \frac{1}{R_{ew}} \left[M - \frac{1}{R_{ew}} E_M^T (L_{1:N,1:N})^{-1} E_M \right]. \quad (10)$$

Since M is assumed to be constant, the only randomness in σ comes from $L_{1:N,1:N}$. Since this matrix is positive definite when the network is connected and is a linear function of A^*,

σ is a concave function of A^*. Jensen's inequality then tells us that for all $\mathcal{X}, \mathcal{Y}, \Theta, \sigma^*$ is an upper bound on $E\sigma$ as shown in Eq. (11):

$$E\sigma(A) = E\sigma(A^*) \leqslant \sigma(EA^*) = \sigma^*. \quad (11)$$

III. MODEL COMPUTATION

A. Methods for computing EA^*

The approximate model σ^* is useful because we can directly compute EA^* in a wide variety of circumstances. This eliminates the need for Monte Carlo sampling of networks and solving a linear system of equations for each sample. Here we present a method for computing EA^* when $\mathcal{X}, \mathcal{Y}$ are the uniform distribution, which is an assumption used throughout the literature. This procedure is applicable for any orientation distribution Θ that can be parameterized by a vector $\boldsymbol{\alpha}$.

Recall that A^* is the sorted adjacency matrix of a random nanowire network and has size $N + 2 \times N + 2$. The first N indices correspond to a nanowire, sorted by increasing x coordinate, while indices $N + 1$ and $N + 2$ correspond to the left and right border electrode. The elements of the expected adjacency matrix EA^* are thus the probability of intersection between the objects of indices i, j. To compute the matrix, we thus need to compute the probability of intersection between every pair of wires, conditioned on the rank of the x coordinate of each wire. We also need to calculate the probability of intersection between each wire and the border electrodes, conditioned on the rank of the x coordinate of the wire. Because the matrix is symmetric, we need to do so only for $i > j$, and we need to do the calculation only for a single border electrode because the probabilities for the other border electrode are symmetric.

We will first calculate the probability of intersection between any two nanowires. Denote a wire as $w = (x, y, \theta)$ and let w_i^*, w_j^* be the ith and jth wire according to the sorted order based on x coordinate. The desired probability is then denoted by $P(w_i^* \cap w_j^*)$. The event of w_i^* intersecting w_j^* is a deterministic function of the difference in x coordinates, the difference in y coordinates, and the angles of the two wires. Under our independence assumptions, we can thus calculate EA_{ij}^* by calculating the distributions of $x_i^* - x_j^*$ and $y_i^* - y_j^*$ and then using the known distributions of θ_i and θ_j. For brevity, we define

$$x_{ij} = x_i^* - x_j^*, \quad (12)$$

$$y_{ij} = y_i^* - y_j^*. \quad (13)$$

We will first analyze randomness solely in y_{ij} by computing the intersection probability conditioned on x_{ij}, denoted by $P(w_i^* \cap w_j^* | x_{ij})$. This is the probability that two wires intersect if we know the difference in x coordinates between them. For any pair of wires w_i^*, w_j^* with x separation x_{ij} and angles θ_i, θ_j, we can define the horizontal range of overlap b as the length of the interval of x coordinates that both wires lie in. For particular values of b, θ_i, θ_j, there is an interval of y_{ij} values for which w_i and w_j will cross. We denote the length of this interval of by h. We illustrate these quantities with example nanowire pair configurations in Fig. 3.
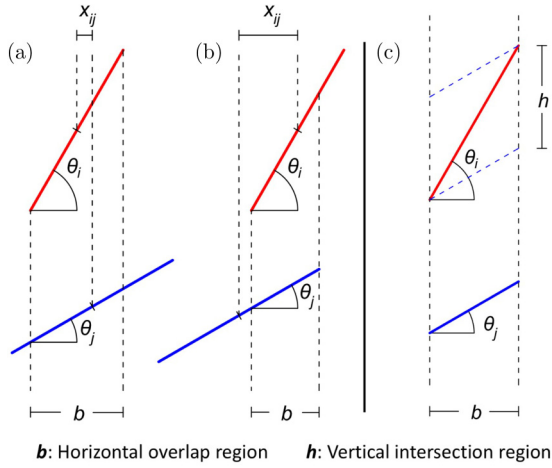
b: Horizontal overlap region   **h**: Vertical intersection region

FIG. 3. If two nanowires have known x separation of x_{ij} and angles θ_i and θ_j, we can calculate the length of the horizontal region of overlap b, which is the length of the x coordinates that both nanowires enter. This quantity is visualized in the case where the horizontal region of one nanowire is contained in the region of the other (a) as well as the case where this is not true (b). We can then use this quantity to calculate the length of the range of y separations h for which the two nanowires would intersect, as visualized in (c).

Now observe that the distribution of y_{ij} is identical for all $i \neq j$. Furthermore, because of our use of periodic boundary conditions, since $\mathcal{Y}$ is the uniform distribution, y_{ij} is in fact the uniform distribution in the range $[0, 1)$. Therefore, the probability of intersection between w_i and w_j conditioned on x_{ij} is given by the conditional expectation of h:

$$P(w_i^* \cap w_j^* | x_{ij}) = E[h | x_{ij}]. \quad (14)$$

We can calculate this conditional expectation by observing that b and h can be calculated from x_{ij} and θ_i, θ_j, as in Eqs. (15) and (16). Here $(f)_+$ is defined to be $\max\{f, 0\}$:

$$b(x_{ij}, \theta_i, \theta_j) = \min \begin{cases} [(l/2)(\cos\theta_i + \cos\theta_j) - x_{ij}]_+ \\ l\cos\theta_i \\ l\cos\theta_j \end{cases}, \quad (15)$$

$$h(x_{ij}, \theta_i, \theta_j) = b(x_{ij}, \theta_i, \theta_j)|\tan\theta_i - \tan\theta_j|. \quad (16)$$

In Eq. (15) the latter two cases correspond to the situation when the interval of x coordinates that one wire lies in is contained by the interval of x coordinates that the other lies in, as in Fig. 3(a). The first case is taken when this situation does not occur, as in Fig. 3(b).

The conditional expectation is then given by integrating out θ_i and θ_j drawn independently from Θ:

$$P(w_i^* \cap w_j^* | x_{ij}) = \int h(x_{ij}, \theta_i, \theta_j) p(\theta_i) p(\theta_j) \, d(\theta_i \theta_j). \quad (17)$$

Since we have assumed the wires are sorted by x coordinate, the difference x_{ij} is the difference in order statistics i and j from the distribution $\mathcal{X}$. Because $\mathcal{X}$ is the uniform distribution, x_{ij} follows the β distribution with parameters $i - j$ and $N - i + j + 1$, if $i > j$ [32]. However, for the networks with large N which we study, these distributions become strongly concentrated at their mean, which is $\frac{i-j}{N+1}$. We thus assume that x_{ij} is equal to its expected value and empirically observe no loss in accuracy. This yields a formula for the probability of

intersection between any two nanowires:

$$P(w_i^* \cap w_j^*) = P\left(w_i^* \cap w_j^* | x_{ij} = \frac{i-j}{N+1}\right). \quad (18)$$

A similar argument can be used to calculate the probability that any wire crosses the left border electrode, denoted by e_1. Observe that w_i^* intersects e_1 if and only if $(l/2)\cos\theta_i \geqslant x_i^*$. Assuming that x_i^* equals its expected value of $\frac{i}{N+1}$, the desired probability is then given by Eq. (19), where $\theta \sim \Theta$:

$$P(x_i^* \cap e_1) = P\left[\cos\theta \geqslant \frac{2i}{l(N+1)}\right]. \quad (19)$$

We can therefore calculate every element of EA^* for any N and any orientation distribution Θ, assuming wire positions are uniform.

To use these expressions efficiently, we numerically compute the integral in Eq. (17) over a grid of values for x_{ij} and the parameters $\boldsymbol{\alpha}$ of the orientation distribution Θ. We then fit a polynomial to the probability values on these grid points to obtain an expression for $P(w_i^* \cap w_j^*)$ that is extremely rapid to use. We further describe the speed of our method in the next subsection.

B. Analysis of computational speed

One of the significant advantages of our method is that it replaces Monte Carlo sampling with an asymptotically faster computation. Sampling-based models, which are the most common approaches for studying random nanowire networks, have two major components. First, a number of nanowire networks M are sampled by directly sampling (x, y, θ) for each of N nanowires, and a collection of M adjacency matrices are calculated. Second, the Kirchhoff current equation is solved for each adjacency matrix to collect M observations of sheet conductivity, and these observations are then averaged. The first of these steps has complexity $O(MN^2)$. Within all networks, each of the N nanowires must be compared with a fixed fraction of all other nanowires for intersection to compute the adjacency matrix A. The second step, meanwhile, has complexity $O(MN^3)$, which is the cost of solving M linear systems of equations each involving N variables. While the second step has larger complexity, both steps require significant amounts of time, and so speeding up either is beneficial.

Our model σ^* delivers a large asymptotic improvement to the first step and delivers a large constant factor improvement to the second step. Recall that the probability of intersection between two wires under our model depends only on the expected x separation between them. As a result, we need only to directly compute two rows of EA^* in order to produce the entire matrix because the expected x separation between the wires w_i^* and w_j^* is determined completely by the quantity $|i - j|$. Equivalently, if we ignore the rows representing electrodes, then all diagonals of EA^* are constant. We therefore must compute the first row of EA^* to obtain the probability of interaction between every pair of nanowires and also must compute the last row of EA^* to obtain the probability of interaction between every nanowire and an electrode. Therefore, the cost of computing EA^* is $O(N)$ with constant proportional to the time it takes to compute $P(w_i^* \cap w_j^*)$. We must still

solve a single Kirchhoff current equation, and this step is $O(N^3)$.

Numerically integrating to compute each evaluation of $P(w_i^* \cap w_j^*)$ is in practice quite slow. We therefore precompute this function for a grid of values of x_{ij} as well the parameters $\boldsymbol{\alpha}$ of the orientation distribution Θ, and then fit a polynomial to the computed values. A polynomial fit is in practice quite accurate because the probability in question is smooth as a function of the parameters of interest. This step makes computation of $P(w_i^* \cap w_j^*)$ extremely rapid, but the precomputation cost is exponential in the number of parameters of the orientation distribution. For the majority of interesting cases, the orientation distribution can be parameterized in one or two parameters, and this complexity is thus not significant compared to other steps.

In total, our method has a small precomputation cost but replaces the $O(MN^2)$ complexity of Monte Carlo sampling with an asymptotically faster $O(N)$ computation. It also reduces the cost of solving linear systems by a factor of M, the number of samples that are collected in a sampling based approach. In our implementation, this allowed the model σ^* to be evaluated about 100 times faster than direct Monte Carlo sampling.

IV. EMPIRICAL TESTS AND DISCUSSION

We examine the effectiveness of σ^* in modeling dependency of network conductivity on both nanowire density and orientation distribution. We assume, as in the previous section, that $\mathcal{X}, \mathcal{Y}$ are both the uniform distribution. We implemented direct sampling of σ under this assumption and our previously stated setting, while allowing the distribution Θ to be arbitrary. We use our implementation of direct sampling of σ as a baseline comparison for all tests, estimating $E\sigma$ with $\hat{\sigma}$ with $M = 30$. Throughout these experiments, we use $l = 0.1$. Larger values of M reduce the noise of $\hat{\sigma}$, while smaller values of l reduce finite size error in $\hat{\sigma}$ and σ^*. The chosen values of M and l were found empirically to be sufficient to largely eliminate these errors; σ^* and $\hat{\sigma}$ do not change much for higher M or lower l, as long as C_N is fixed.

A. Dependence on nanowire density

We first assume that Θ is the isotropic distribution (uniform in $[-90, 90]$ degrees) and explore the dependence of σ^* on normalized concentration C_N. Figure 4 shows a comparison between normalized σ^* and $\hat{\sigma}$ as a function of C_N, starting just above the percolation threshold, on both linear and double log scales. Conductivities are normalized by multiplying by junction resistance 1Ω so that they are unitless. It is a known result that $E\sigma$ can be approximated as a power-law function of the distance of normalized concentration from the percolation threshold, with an exponent of around 1.75 at medium densities which moves close to 2 at high densities [9]. Our estimate $\hat{\sigma}$ matches these known relationships; the growth pattern of conductivity in log space becomes linear as the subtraction of the percolation threshold becomes negligible. Our model σ^*, however, displays a perfect power-law dependence on C_N, with an exponent that matches the asymptotic exponent of $E\sigma$. Near the percolation threshold, the error is large, as we have
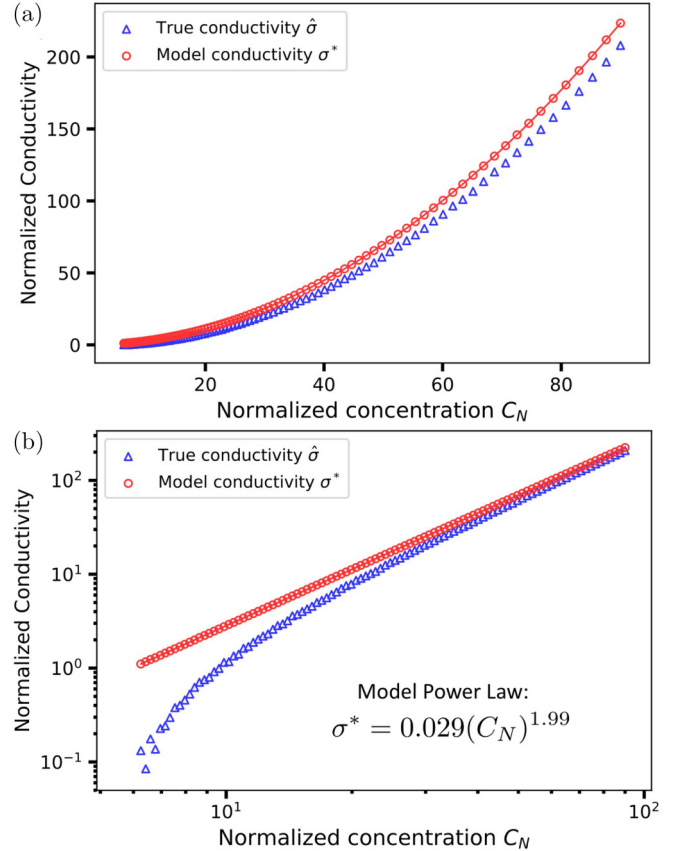

FIG. 4. Normalized conductivity as a function of normalized wire concentration is shown for both the true empirical mean and our approximate analytical model, on a linear scale (a) and a double log scale (b). The model follows an exact power-law relationship and corresponds to the high-density behavior of the true conductivity. We emphasize that the model is not obtained by fitting to the true conductivity.

assumed nanowire density above this threshold in developing our model. However, the error in log space approaches zero as concentration grows, and the model can thus be interpreted as the limiting behavior of $E\sigma$ at high concentrations.

While σ^* is less precise than other recent models for predicting dependency of conductivity on concentration at small nanowire densities, the result that our approach yields the correct limiting behavior is theoretically interesting. By using EA^*, our model directly encodes clustering of nanowire only in the x direction. However, this is sufficient information to capture asymptotic behavior and, as we next show, capture the effect of varying orientation distribution.

B. Dependence on orientation distribution

Our model σ^* is particularly valuable because it is able to predict the effect of arbitrary orientation distributions on sheet conductivity. The problem of optimizing orientation distribution in random nanowire networks has been studied numerous times via computational models, but there is no unified understanding of the observed effects [10,11,13,14,16].

We consider two families of distributions for Θ, each of which is described by a single parameter. For each family, we
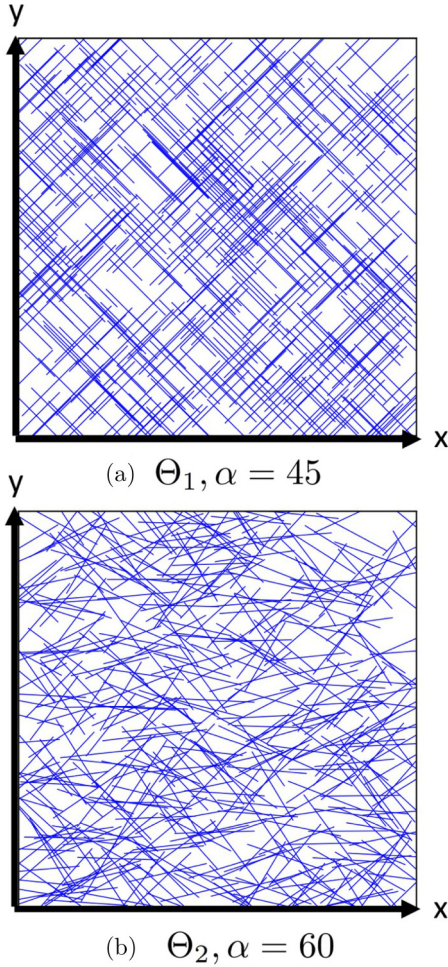
(a) $\Theta_1, \alpha = 45$

(b) $\Theta_2, \alpha = 60$

FIG. 5. Nanowire networks drawn from (a) Θ_1, with $\alpha = 45$ and (b) Θ_2, with $\alpha = 60$ are shown. In Θ_1, all nanowires have orientation at $\pm\alpha$ degrees from the horizontal (x direction). In Θ_2, nanowire orientation is distributed uniformly in $[-\alpha, \alpha]$ degrees from the horizontal.
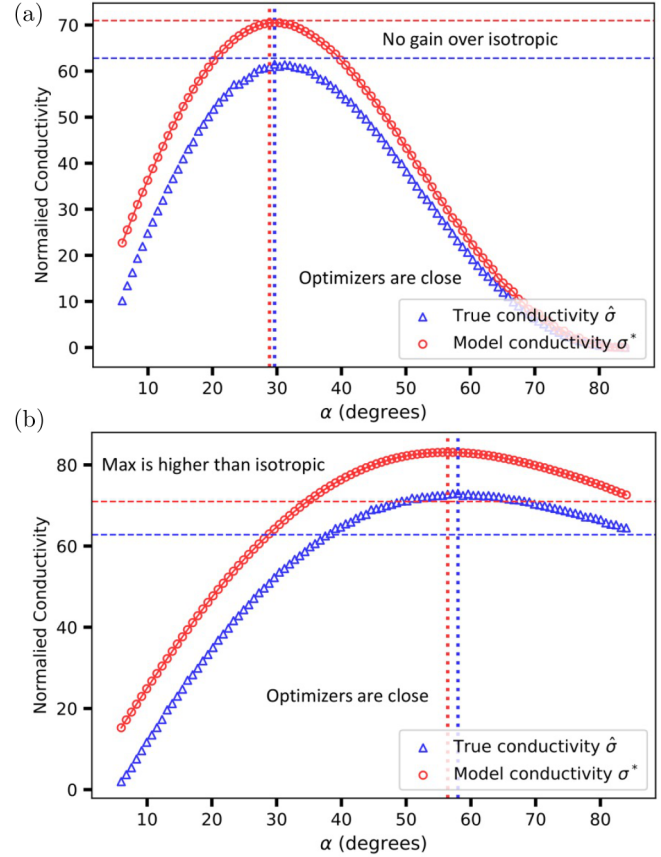

FIG. 6. Normalized conductivity is shown as a function of distribution parameter α for both the true empirical conductivity and the approximate analytical model, for both (a) Θ_1 and (b) Θ_2, with $C_N = 50$. In both families, the shapes of the two curves match well and the optimal values (vertical lines) are close. The model also captures the fact that a gain over isotropic conductivity (horizontal lines) can be achieved only in Θ_2.

demonstrate that σ^* accurately captures the effect of varying the distribution parameter on conductivity. The first family $\Theta_1(\alpha)$ is given by

$$p(\theta) = \begin{cases} \frac{1}{2} & \theta = \alpha \\ \frac{1}{2} & \theta = -\alpha \end{cases} \qquad (20)$$

for all $0 < \alpha < 90$. All probability mass is concentrated at $\pm\alpha$ degrees from horizontal. The second family $\Theta_2(\alpha)$ is given by

$$p(\theta) = \begin{cases} \frac{1}{2\alpha} & |\theta| < \alpha \\ 0 & \text{o.w.} \end{cases} \qquad (21)$$

Probability density is uniformly distributed over $[-\alpha, \alpha]$ degrees. Figure 5 shows a sample network from a single distribution within each family. These two families were previously studied, and it was found that while a conductivity gain over isotropic networks could be achieved within Θ_2, no gain could be achieved within Θ_1 [10].

Figure 6 shows a comparison between σ^* and $\hat{\sigma}$ for determining the relationship between distribution parameter α and normalized conductivity for both Θ_1 and Θ_2. The normalized

concentration is fixed at 50 in both cases. Within both families, the shape of the curve matches well, and the optimal values are within a few degrees of each other. Moreover, the predictions from σ^* match $E\sigma$ in that a gain over isotropic orientation is attainable in Θ_2 but not Θ_1.

To the best of our knowledge, our model is the first to accurately reproduce the effects of orientation distribution on sheet conductivity without relying on Monte Carlo sampling in any capacity. These results indicate that orientation effects can be modeled by analyzing their effects on network connectivity in a single direction, as our model A^* takes into account positions of nanowires only in the x direction.

V. CONCLUSION

We developed an approximate analytical model for sheet conductivity of random nanowire networks that condenses a large amount of their structure through a specific choice of nanowire permutation. We showed that this model is an upper bound and matches the asymptotic dependency of the true sheet conductivity on wire concentration. We also demonstrated that the model accurately captures the effects of orientation on nanowire network conductivity, a result

that has limited theoretical explanation in the literature. Our model accurately captures the effects of arbitrary orientation distributions on network conductivity and replaces Monte Carlo sampling with an asymptotically faster computation. These results and the structure of the model we developed provide theoretical intuition about random nanowire network conductivity. Namely, our results demonstrate that network connectivity in the direction of current flow is the key factor in determining the dependence of conductivity on wire density and orientation distribution, because our model encodes connectivity information only in the x direction.

The most pressing direction for future research is to relax our assumption of zero wire resistance, as recent work has indicated that the junction resistance in silver nanowire networks can be reduced to a comparable magnitude as the wire resistance [18]. This could be done, for example, by using an approximate function to calculate sheet conductivity based on EA^* in the presence of wire resistance. Various recent analytical models for random nanowire network conductivity have successfully used approximations about the number of nanowires that a given nanowire will intersect [25,29]. Rather than using approximations derived in the setting of uniform wire orientation, these models could instead use approximations obtained from EA^* for an arbitrary orientation distribution. The success of these existing models indicates that they would likely function as accurate approximate functions to calculate sheet conductivity given the information in EA^*.

[1] A. Kumar and C. Zhou, ACS Nano **4**, 11 (2010).

[2] R. G. Gordon, MRS Bull. **25**, 52 (2000).

[3] S. Choi, S. I. Han, D. Kim, T. Hyeon, and D.-H. Kim, Chem. Soc. Rev. **48**, 1566 (2019).

[4] D. S. Hecht, L. Hu, and G. Irvin, Adv. Mater. **23**, 1482 (2011).

[5] L. Hu, H. Wu, and Y. Cui, MRS Bull. **36**, 760 (2011).

[6] J.-Y. Lee, S. T. Connor, Y. Cui, and P. Peumans, Nano Lett. **8**, 689 (2008).

[7] A. Teymouri, S. Pillai, Z. Ouyang, X. Hao, F. Liu, C. Yan, and M. A. Green, ACS Appl. Mater. Interf. **9**, 34093 (2017).

[8] M. Marus, A. Hubarevich, H. Wang, A. Stsiapanau, A. Smirnov, X. W. Sun, and W. Fan, Opt. Express **23**, 26794 (2015).

[9] R. M. Mutiso, M. C. Sherrott, A. R. Rathmell, B. J. Wiley, and K. I. Winey, ACS Nano **7**, 7654 (2013).

[10] M. Jagota and N. Tansu, Sci. Rep. **5**, 10219 (2015).

[11] A. Behnam, J. Guo, and A. Ural, J. Appl. Phys. **102**, 044313 (2007).

[12] A. Behnam and A. Ural, Phys. Rev. B **75**, 125432 (2007).

[13] F. Du, J. E. Fischer, and K. I. Winey, Phys. Rev. B **72**, 121404(R) (2005).

[14] S. I. White, B. A. DiDonna, M. Mu, T. C. Lubensky, and K. I. Winey, Phys. Rev. B **79**, 024301 (2009).

[15] Y. Y. Tarasevich, I. V. Vodolazskaya, A. V. Eserkepov, V. A. Goltseva, P. G. Selin, and N. I. Lebovka, J. Appl. Phys. **124**, 145106 (2018).

[16] N. Pimparkar, C. Kocabas, S. J. Kang, J. Rogers, and M. A. Alam, IEEE Electron Device Lett. **28**, 593 (2007).

[17] J. Hicks, J. Li, C. Ying, and A. Ural, J. Appl. Phys. **123**, 204309 (2018).

[18] A. T. Bellew, H. G. Manning, C. Gomes da Rocha, M. S. Ferreira, and J. J. Boland, ACS Nano **9**, 11422 (2015).

[19] T. Ackermann, R. Neuhaus, and S. Roth, Sci. Rep. **6**, 34289 (2016).

[20] M. Marus, A. Hubarevich, R. J. W. Lim, H. Huang, A. Smirnov, H. Wang, W. Fan, and X. W. Sun, Opt. Mater. Express **7**, 1105 (2017).

[21] F. Wu, Z. Li, F. Ye, X. Zhao, T. Zhang, and X. Yang, J. Mater. Chem. C **4**, 11074 (2016).

[22] M. Marus, A. Hubarevich, H. Wang, Y. Mukha, A. Smirnov, H. Huang, W. Fan, and X. W. Sun, Thin Solid Films **626**, 140 (2017).

[23] D. Kim and J. Nam, J. Appl. Phys. **124**, 215104 (2018).

[24] Y. Y. Tarasevich, I. V. Vodolazskaya, A. V. Eserkepov, and R. K. Akhunzhanov, J. Appl. Phys. **125**, 134902 (2019).

[25] C. Forró, L. Demkó, S. Weydert, J. Vörös, and K. Tybrandt, ACS Nano **12**, 11080 (2018).

[26] H. G. Manning, C. G. da Rocha, C. O'Callaghan, M. S. Ferreira, and J. J. Boland, Sci. Rep. **9**, 1 (2019).

[27] A. Ponzoni, Appl. Phys. Lett. **114**, 153105 (2019).

[28] R. Benda, E. Cancès, and B. Lebental, J. Appl. Phys. **126**, 044306 (2019).

[29] A. Kumar, N. Vidhyadhiraja, and G. U. Kulkarni, J. Appl. Phys. **122**, 045101 (2017).

[30] D. Stauffer and A. Aharony, *Introduction to Percolation Theory* (Taylor & Francis, Philadelphia, 2018).

[31] D. J. Klein and M. Randić, J. Math. Chem. **12**, 81 (1993).

[32] H. Weisberg, Ann. Math. Stat. **42**, 704 (1971).